# Prediction of compressive strength of slag concrete using a blended cement hydration model

Wang Xiao-Yong[1] and Lee Han-Seung[*2]

[1]*Department of Architectural Engineering, Kangwon National University, Chuncheon, Korea*
[2]*School of Architecture & Architectural Engineering, Hanyang University, Ansan, Korea*

**Abstract.** Partial replacement of Portland cement by slag can reduce the energy consumption and $CO_2$ emission therefore is beneficial to circular economy and sustainable development. Compressive strength is the most important engineering property of concrete. This paper presents a numerical procedure to predict the development of compressive strength of slag blended concrete. This numerical procedure starts with a kinetic hydration model for cement–slag blends by considering the production of calcium hydroxide in cement hydration and its consumption in slag reactions. Reaction degrees of cement slag are obtained as accompanied results from the hydration model. Gel-space ratio of hardening slag blended concrete is determined using reaction degrees of cement and slag, mixing proportions of concrete, and volume stoichiometries of cement hydration and slag reaction. Furthermore, the development of compressive strength is evaluated through Powers' gel-space ratio theory considering the contributions of cement hydration and slag reaction. The proposed model is verified through experimental data on concrete with different water-to-binder ratios and slag substitution ratios.

**Keywords:** slag; hydration model; compressive strength; microstructure; concrete

## 1. Introduction

Granulated slag is produced by quenching the liquid slag with a large amount of water to produce sand-like granulates. The granulates normally contain more than 95% of glass. Generally, they are ground to fine powder, called ground granulated blast furnace slag (GGBS). Using ground granulated blast furnace slag as a supplementary cementitious material in Portland cement concrete has many advantages, including improved durability, workability and economic benefits (Islam *et al*. 2014).

Compressive strength is the most important engineering property of concrete. Many experimental studies have been done about the development of compressive strength of slag blended concrete. Cheng *et al*. (2008) investigated strength development of slag blended concrete with different water to binder ratios and slag replacement ratios. Under standard curing conditions, at early age, slag blended concrete gain strength more slowly than Portland cement concrete. However, at late age, strength of slag blended concrete can surpass that of Portland cement

---

∗Corresponding author, Professor, E-mail: ercleehs@hanyang.ac.kr

concrete. Barnett *et al.* (2006) made experimental investigations on strength development of mortars containing ground granulated blast-furnace slag and Portland cement. Variables were the level of slag in the binder, water–binder ratio and curing temperature. They found that the early age strength is much more sensitive to temperature for higher levels of slag and the apparent activation energy increases approximately linearly with slag level. Oner and Akyuz (2007) presented a laboratory investigation on optimum level of ground granulated blast-furnace slag on the compressive strength of concrete. The test results proved that the compressive strength of concrete mixtures containing GGBS increases as the amount of GGBS increase. After an optimum point, at around 50% of the total binder content, the addition of GGBS does not improve the compressive strength. From references (Cheng *et al.* 2008; Barnett *et al.* 2006; Oner and Akyuz, 2007), it can be seen that the mechanical properties of slag blended concrete relate with both cement hydration and slag reaction. The development of compressive strength depends on many factors, such as age, water to binder ratio, slag replacement ratio, and curing conditions.

On the other hand, some models have been proposed to evaluate properties of hardening slag blended concrete. Douglas and Pouskouleli (1991) put forward a statistical design to describe the strength development of Portland cement-slag-fly ash mortars at various ages. With the experimental compressive strength values, a computerized statistical approach was used to find the equations governing strength development of the ternary systems at different ages. Brooks and Kaisi (1990) proposed a model to evaluate the early strength development of Portland and slag cement concretes cured at elevated temperatures. The development of strength under isothermal conditions was described by a hyperbolic expression equation, and the strength development for heat-cycled cured concrete was described using an equivalent isothermal temperature.

Contrasting to the empirical models of strength development of slag blended concrete (Douglas and Pouskouleli 1991; Brooks and Kaisi 1990), some hydration models have been built to predict mechanical-thermal-chemical-hydro properties of hardening slag blended concrete. Based on an extensive experimental research program on hardening slag blended concrete elements, De Schutter and Taerwe (1996) proposed a degree of hydration-based description for the compressive strength, Young's modulus, the uniaxial tensile strength, the splitting tensile strength, the flexural tensile strength, Poisson's ratio and the peak strain. Based on a multi-component hydration heat model and micro pore structure formation model, Song and Kwon (2009) evaluated chloride penetration in silica fume, fly ash and slag blended concrete using the diffusion coefficients obtained from a neural network algorithm. Similar with Song and Kwon (2009), based on computed micro pore structure, Yoon (2009) proposed a simple approach to calculate the diffusivity of concrete considering effects of tortuosity, micro-structural properties of hardened cement paste, and volumetric portion of aggregate. Most recently, Luan *et al.* (2012) proposed a hydration model of slag blended cement considering the role of calcium hydroxide as activator and the Ca/Si ratio of CSH. The influence of low Ca/Si ratio in the CSH inner product on slag reaction was taken into account using an enhanced slag reaction model. From references (De Schutter and Taerwe 1996; Song and Kwon 2009; Yoon 2009; Luan *et al.* 2012), it can be seen that, based on the hydration model, the evolution of properties of hydrating cementitious materials can be described kinetically.

Due to the reaction between cement hydration and slag reaction, compared with ordinary Portland cement, the hydration of cement blended with slag is much more complex. As proposed by Luan *et al.* (2012), it is typical to consider the hydration reactions of cement and the blended mineral admixtures to model the hydration of blended concrete. In this paper, a numerical model is proposed to simulate the hydration of concrete containing slag. By considering the production of

dkfmadkcalcium hydroxide in cement hydration and its consumption during the reaction of mineral admixture, the reaction of slag is separated from that of cement hydration. The compressive strength development of hardening slag blended concrete is evaluated based on degree of hydration of cement and reaction degree of slag.

The contribution of this paper is relating the macro mechanical properties, i.e., development of compressive strength of blended concrete, with the evolution of microstructure of cement-slag blends. The parameters of cement hydration model, slag reaction model, and compressive strength development model are not changed when water to binder ratios and slag replacement ratios vary from one mix to the other. The physical meaning of these parameters is clear. Using the proposed calibration process in this paper, it is convenient for other researchers to use this hydration model. In addition, Oner and Akyuz (2007) reported that for concrete incorporating slag, after an optimum slag content, the addition of slag does not improve the compressive strength of concrete. In this paper, because the proposed model has taken into account the effect of slag replacement ratio on strength development, the proposed model can predict compressive strength development of concrete incorporating different slag contents. Furthermore, by comparing the strength development of slag blended concrete with that of Portland cement concrete, the optimum slag content can be analyzed.

## 2. Hydration model of portland cement

Tomosawa (1997) proposed a shrinking-core model to model the hydration of Portland cement. This model is expressed as a single equation consisting of three coefficients: $k_d$ the reaction coefficient in the induction period; $D_e$ the effective diffusion coefficient of water through the C–S–H gel; and $k_{ri}$ a coefficient of the reaction rate of mineral compound of cement as shown in eqs. (1-1) and (1-2) below:

$$\frac{d\alpha_i}{dt} = \frac{3\left(S_w / S_0\right)\rho_w C_{w-free}}{(v + w_g)r_0\rho_c} \cdot \frac{1}{(\frac{1}{k_d} - \frac{r_0}{D_e}) + \frac{r_0}{D_e}(1-\alpha_i)^{\frac{-1}{3}} + \frac{1}{k_{ri}}(1-\alpha_i)^{\frac{-2}{3}}} \tag{1-1}$$

$$\alpha = \frac{\sum_{i=1}^{4}\alpha_i g_i}{\sum_{i=1}^{4} g_i} \tag{1-2}$$

where $\alpha_i$ ($i$ = 1,2,3, and 4) represents reaction degree of mineral compound of cement $C_3S$, $C_2S$, $C_3A$, and $C_4AF$ respectively; $\alpha$ is the degree of cement hydration and can be calculated from the weight fraction of mineral compound $g_i$ and reaction degree of mineral compound $\alpha_i$; $v$ is the stoichiometric ratio by mass of water to cement (= 0.25); $w_g$ is the physically bound water in C–S–H gel (= 0.15); $\rho_w$ is the density of water; $\rho_c$ is the density of the cement; $C_{w-free}$ is the amount of water at the exterior of the C–S–H gel; $r_0$ is the radius of unhydrated cement particles; $S_w$ is the effective surface area of the cement particles in contact with water; and $S_0$ is the total surface area if the surface area develops unconstrained.

The reaction coefficient $k_d$ is assumed to be a function of the degree of hydration as shown in Eq. (2) where *B* and *C* are the coefficients determining this factor; *B* controls the rate of the initial shell formation and *C* controls the rate of the initial shell decay.

$$k_d = \frac{B}{\alpha^{1.5}} + C\alpha^3 \tag{2}$$

The effective diffusion coefficient of water is affected by the tortuosity of the gel pores as well as the radii of the gel pores in the hydrate. This phenomenon can be described as a function of the degree of hydration and is expressed as follows:

$$D_e = D_{e0} \ln(\frac{1}{\alpha}) \tag{3}$$

In addition, free water in the capillary pores is depleted as hydration of cement minerals progresses. Some water is bound in the gel pores, and this water is not available for further hydration, an effect that must be taken into consideration in every step of the progress of the hydration. Therefore, the amount of water in the capillary pores $C_{w-free}$ is expressed as a function of the degree of hydration in the previous step as shown in Eq. (4).

$$C_{w-free} = \frac{W_0 - 0.4 * \alpha * C_0}{W_0} \tag{4}$$

where $C_0$ and $W_0$ are the mass fractions of cement and water in the mix proportion.

The effect of temperature on these reaction coefficients is assumed to follow Arrhenius's law as shown in Eqs. (5)–(8):

$$B = B_{20} \exp(-\beta_1(\frac{1}{T} - \frac{1}{293})) \tag{5}$$

$$C = C_{20} \exp(-\beta_2(\frac{1}{T} - \frac{1}{293})) \tag{6}$$

$$k_{ri} = k_{ri20} \exp(-\frac{E}{R}(\frac{1}{T} - \frac{1}{293})) \tag{7}$$

$$D_e = D_{e20} \exp(-\beta_3(\frac{1}{T} - \frac{1}{293})) \tag{8}$$

where $\beta_1, \beta_2, E/R$, and $\beta_3$ are temperature sensitivity coefficients and $B_{20}$, $C_{20}$, $k_{ri20}$, and $D_{e20}$ are the values of $B, C, k_{ri}$, and $D_e$ at 20°C.

On the basis of degree of reactions of mineral compounds of cement (Matsushita *et al.* 2007), the parameters of hydration model are calibrated and shown in Table 1. The comparison between the experimental results and the prediction results are shown in Fig. 1. Because the reaction rate of C₃S and C₃A is much quicker than C₂S and C₄AF, the hydration of C₃S and C₃A reaches a steady state much earlier than C₂S and C₄AF. Most of C₃A and C₃S have reacted in the first 1000 h. As shown in Fig. 1, the prediction results agree well overall with the experimental results. On
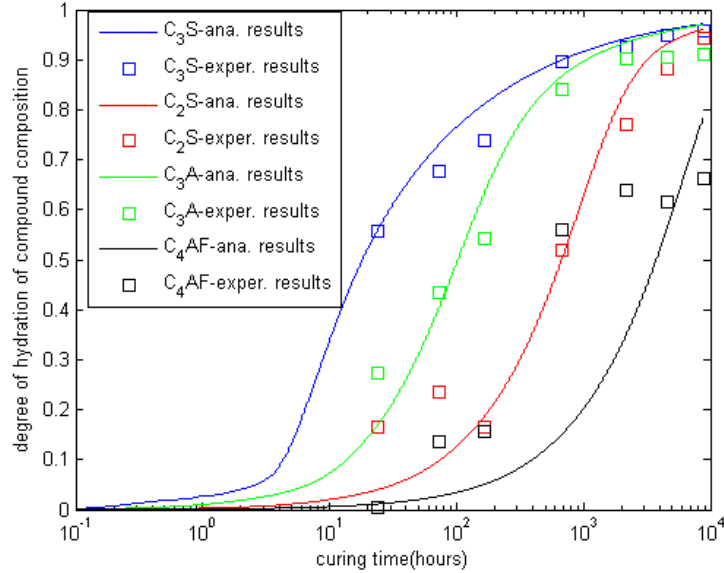
Fig. 1 reaction degree of mineral compounds of cement (water to cement ratio 0.5, curing temperature 20℃)

Table 1 Coefficients of cement hydration model

| $B_{20}$ (cm/h) | $C_{20}$ (cm/h) | $k_{rC_3S20}$ (cm/h) | $k_{rC_2S20}$ (cm/h) | $k_{rC_3A20}$ (cm/h) | $k_{rC_4AF20}$ (cm/h) | $D_{e20}$ (cm²/h) | $\beta_1$ (K) | $\beta_2$ (K) | $\beta_3$ (K) | $\dfrac{E}{R}$ (K) |
|---|---|---|---|---|---|---|---|---|---|---|
| $8.09\times10^{-9}$ | 0.02 | $9.03\times10^{-6}$ | $2.71\times10^{-7}$ | $1.35\times10^{-6}$ | $6.77\times10^{-8}$ | $8.62\times10^{-10}$ | 1000 | 1000 | 7500 | 5400 |

the other hand, it should be noticed that Tomosawa's model is valid only for Portland cement. For slag blended cement, due to the coexisting of Portland cement hydration and chemical reaction of slag, Tomosawa's model is not valid. To model the hydration of slag blended concrete, the reaction model of slag should be built and the mutual interactions between cement hydration and slag reaction should be clarified.

## 3. Hydration model for slag blended cement

### 3.1 Amount of calcium hydroxide (CH) during the hydration process

Based on analysis of the experimental results of the amount of chemically bound water, adiabatic temperature rise, and temperature measurement of small quasi-adiabatic blocks, Maekawa *et al*. (2009) said that the reaction of slag can be roughly described by the following approximate key figures:
Calcium hydroxide                    0.22 g/g slag

Chemically bound water               0.30 g/g slag
Gel water                            0.15 g/g slag
Using the hydration model and the stoichiometry of the reaction of slag proposed by Maekawa *et al.* (2009), the amounts of calcium hydroxide, chemically bound water, and capillary water in cement-slag blends during hydration can be determined with the following equations:

$$CH = RCH_{CE} * C_0 * \alpha - RCH_{SG} * \alpha_{SG} * P \tag{9}$$

$$W_{cap} = W_0 - 0.4 * C_0 * \alpha - RCW_{SG} * \alpha_{SG} * P - RPW_{SG} * \alpha_{SG} * P \tag{10}$$

$$W_{cbm} = v * C_0 * \alpha + RCW_{SG} * \alpha_{SG} * P \tag{11}$$

In Eqs. (9), (10) and (11), CH, $W_{cap}$, and $W_{cbm}$ are the masses of calcium hydroxide, capillary water, and chemically bound water, respectively; $\alpha_{SG}$ is degree of reaction of slag; $P$ is the mass of slag in the mixture proportion; $RCH_{CE}$ is the mass of produced calcium hydroxide from the hydration of cement; $RCH_{SG}$ is the mass of reacted calcium hydroxide in the reaction of slag; $RCW_{SG}$ is the mass of chemically bound water in the reaction of slag; and $RPW_{SG}$ is the mass of gel water in the reaction of slag. As shown in Eqs. (9)-(11), the evolution of calcium hydroxide, chemically bound water, and capillary water in cement-slag blends depends on both cement hydration and slag reaction.

## 3.2 Simulation of the slag reaction in slag blended cement

The hydration rate of slag depends on the amount of calcium hydroxide in hydrating cement-slag blends and the reaction degree of mineral admixtures (Tomosawa 1997; Han *et al.* 2003). Compared with the silica fume, the hydration rate of the slag is much lower levels due to the larger particle size. In the simulation, it is assumed that the reaction of slag is divided into three processes: an initial dormant period, and phase-boundary reaction and diffusion processes. By considering these points, based on the method proposed by Saeki and Monteiro (2005), the reaction equation of slag can be written as follows:

$$\frac{d\alpha_{SG}}{dt} = \frac{m_{CH}(t)}{P} \frac{W_{cap}}{W_0} \frac{3\rho_w}{v_{SG} r_{SG0} \rho_{SG}} \frac{1}{(\frac{1}{k_{dSG}} - \frac{r_{SG0}}{D_{eSG}}) + \frac{r_{SG0}}{D_{eSG}}(1-\alpha_{SG})^{\frac{-1}{3}} + \frac{1}{k_{rSG}}(1-\alpha_{SG})^{\frac{-2}{3}}} \tag{12-1}$$

$$k_{dSG} = \frac{B_{SG}}{(\alpha_{SG})^{1.5}} + C_{SG} * (\alpha_{SG})^3 \tag{12-2}$$

$$D_{eSG} = D_{eSG0} * \ln(\frac{1}{\alpha_{SG}}) \tag{12-3}$$

where $m_{CH}(t)$ is the calcium hydroxide mass in a unit volume of hydrating cement-slag blends and can be obtained from Eq. (9); $v_{SG}$ is the stoichiometric ratio of the mass of CH to slag; $r_{SG0}$

is the radius of the slag particle; $\rho_{SG}$ is the density of the slag; $k_{dSG}$ is the reaction rate coefficient in the dormant period ($B_{SG}$ and $C_{SG}$ are coefficients); $D_{eSG0}$ is the initial diffusion coefficient; and $k_{rSG}$ is the reaction rate coefficient.

The influence of temperature on slag reaction is considered by the Arrhenius law as follows:

$$B_{SG} = B_{SG20} \exp(-\beta_{1SG}(\frac{1}{T} - \frac{1}{293}))$$

(12-4)

Setting of initial conditions and calculating time, $t_{end}$

$t = t + \Delta t$

Hydration model:

$\Delta\alpha = f_{ce}(T,t); \Delta\alpha_{SG} = f_{SG}(T,t)$

Calculating a degree of hydration:

$\alpha = \alpha + \Delta\alpha; \; \alpha_{SG} = \alpha_{SG} + \Delta\alpha_{SG}$

The amount of calcium hydroxide:

$CH = RCH_{CE} * C_0 * \alpha - RCH_{SG} * \alpha_{SG} * P$

The amount of capillary water:

$W_{cap} = W_0 - 0.4 * C_0 * \alpha - RCW_{SG} * \alpha_{SG} * P - RPW_{SG} * \alpha_{SG} * P$

The amount of chemically bound water:

$W_{cbm} = v * C_0 * \alpha + RCW_{SG} * \alpha_{SG} * P$

The amount of gel-space ratio and compressive strength:
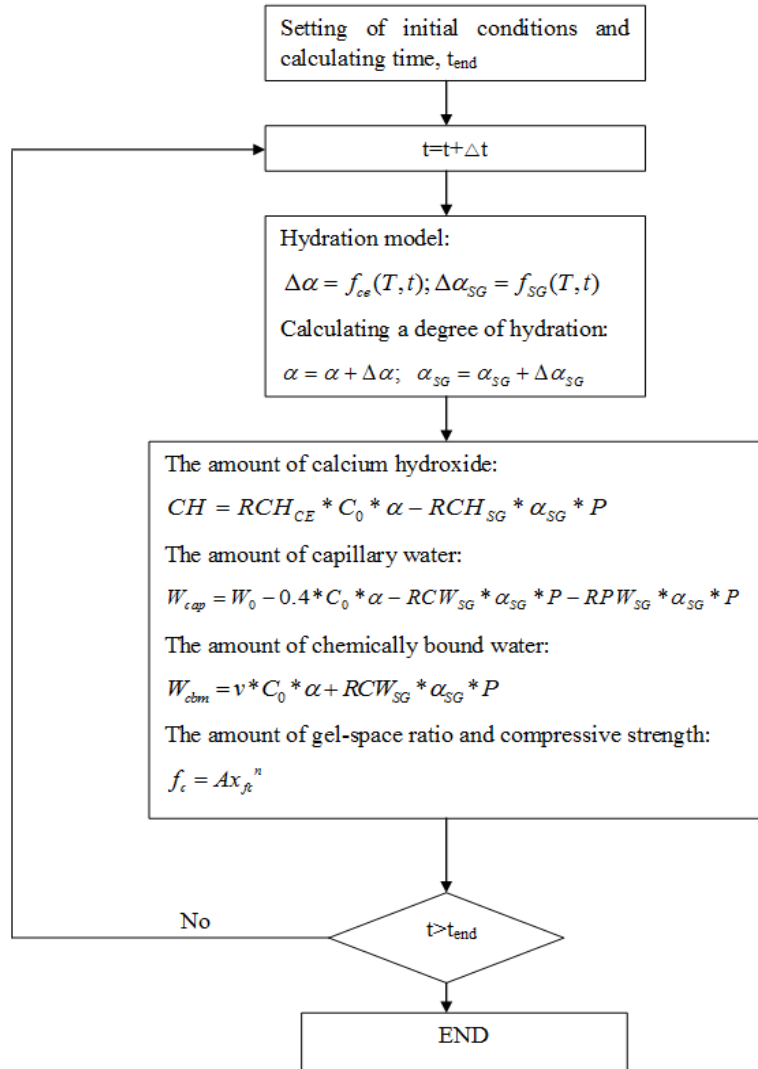
$f_c = Ax_{ft}^n$

No

$t > t_{end}$

END

Fig. 2 flowchart of modeling

$$C_{SG} = C_{SG20} \exp(-\beta_{2SG}(\frac{1}{T} - \frac{1}{293})) \tag{12-5}$$

$$D_{eSG0} = D_{eSG20} \exp(-\beta_{3SG}(\frac{1}{T} - \frac{1}{293})) \tag{12-6}$$

$$k_{rSG} = k_{rSG20} \exp(-\frac{E_{SG}}{R}(\frac{1}{T} - \frac{1}{293})) \tag{12-7}$$

where $B_{SG20}$, $C_{SG20}$, $D_{eSG20}$, and $k_{rSG20}$ are the values of $B_{SG}$, $C_{SG}$, $D_{eSG0}$, and $k_{rSG}$ at 293 K, respectively, and $\beta_{1SG}, \beta_{2SG}, \beta_{3SG}$, and $E_{SG}/R$ are the temperature sensitivity coefficients of $B_{SG}$, $C_{SG}$, $D_{eSG0}$, and $k_{rSG}$, respectively.

When slag is incorporated in concrete, two possible reasons may be adopted to explain the change in hydration process. One is the chemical reaction of amorphous phases in slag, and the other is the influence of slag on the hydration of cement hydration. In the current paper, the new model is proposed which can describe the reaction of slag. On the other hand, the influence of slag on hydration of cement is considered through the amount of capillary water (Eq.(10)) and the dilution effect (Eq. (4)) (Maekawa *et al.* 2009) . Hence the proposed model shows a strong ability to simulate the hydration of concrete containing slag. Furthermore, the development of properties of hardening slag blended concrete can be evaluated based on the degree of reactions of cement and slag.

The flowchart of modeling is shown in Fig. 2. The proposed procedure has considered the effects of slag replacement ratios, water to binder ratios, and curing temperatures on the hydration of slag blended concrete. At each time step, the calcium hydroxide contents, capillary water contents, chemically bound water contents, gel-space ratio, and compressive strength of hardening slag blended concrete are determined using cement hydration degree and slag reaction degree.

### 3.3 Calibration of reaction coefficients of slag reaction model

Iyoda *et al.* (2011) made an experimental research on the reaction degrees of slag in cement-slag paste at different curing temperatures (5℃, 20℃ and 40℃) and different slag replacement ratios (42% and 67% mass fractions). The water to binder ratio of cement-slag paste is 0.5. A selective dissolution method was used in quantifying the degree of slag reaction at different ages (1 day, 3days, 7days, 28 days, 56 days, and 91 days). The slag reaction ratio was measured by the selective dissolution method using salicylate acid–acetone–methanol solution. The grained sample (0.5 g) was mixed with salicylate acid (2.5 g), acetone (35 ml) and methanol (15 ml) for 1 hour, then allowed to sit for 23 hours. The ratio of slag hydration was calculated from the result for quantity of an-hydrated slag. The accuracy of selective dissolution method for determining the reaction degree of mineral admixture has been verified by Lumley *et al.* (1996) and Tang (2010). The quantity of chemically bound water was determined as the ignition loss at 1050℃ of cement-slag blends.

By using the reaction degrees of slag, the reaction coefficients of slag $B_{SG}$, $C_{SG}$, $D_{eSG}$, and $k_{rSG}$ at different curing temperatures can be calibrated. Furthermore, on the basis of reaction

coefficients at different curing temperatures, the temperature sensitivity coefficients of $B_{SG}$, $C_{SG}$, $D_{eSG}$, and $k_{rSG}$ can be determined. The values of slag reaction coefficients and the temperature sensitivity coefficients are shown in Table 2. These fit parameters for slag are not changed from one mix to the other. The comparison between the analysis results and experimental results are shown in Fig. 3. As shown in this figure, when the curing temperature increases from 5℃ to 40℃, the reaction degrees of slag increase approximately 35 percents. On the other hand, when the replacement ratio of slag increases from 42% (Fig. 3a) to 67% (Fig. 3b), due to the shortage of calcium hydroxide or available space of reaction products, the reaction degrees of slag will decrease significantly. In addition, it should be noticed that the slag hydration rate is far lower than that of Portland cement. As shown in Fig. 3-a, when water to binder ratio is 0.5 and slag replacement ratio is 42%, after three months curing at 20℃, only 60% slag has reacted while at the same age, 90% of Portland cement has hydrated in the slag blended cement paste (Maekawa *et al*. 2009).

The hydration of cement is a highly nonlinear system with complex interactions. To validate the proposed model, multiple checks, including not only the reaction degree of slag but also the evolution of chemically bound water, are carried out for verification. The evaluation of chemically bound water of hardening cement-slag blends with different curing temperatures is shown in Fig. 4.

As shown in this figure, a substantial increase in the amount of bound water occurs ever after several weeks for paste with 5℃ curing temperature (Fig. 4a) whereas, for 40℃ curing temperature (Fig. 4c), due to the acceleration of both cement hydration and slag reaction, the reaction essentially stop after about four weeks.



(a) cement-slag paste with 42% slag    (b) cement-slag paste with 67% slag
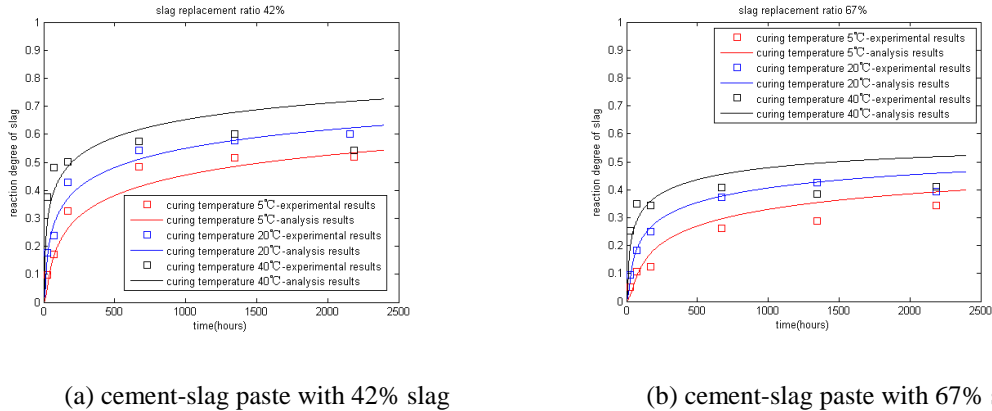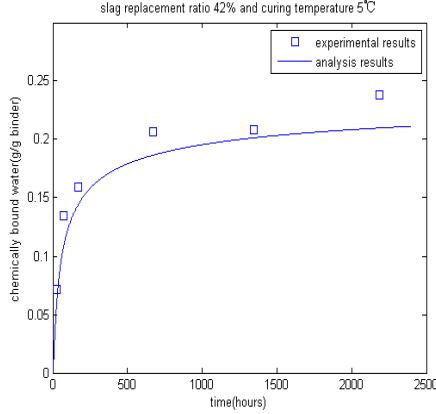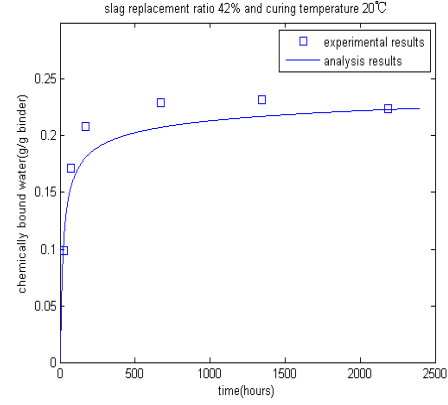
Fig.3 reaction degree of slag with different slag replacement ratios and curing temperatures
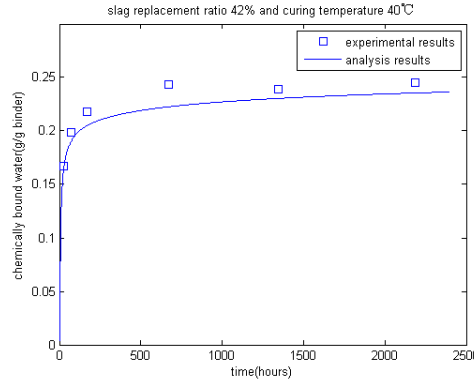
Table 2 Coefficients of slag reaction model

| $B_{20SG}$ (cm/h) | $C_{SG20}$ (cm/h) | $k_{rSG20}$ (cm/h) | $D_{eSG20}$ (cm²/h) | $\beta_{1SG}$ (K) | $\beta_{2SG}$ (K) | $\beta_{3SG}$ (K) | $\dfrac{E_{SG}}{R}$ (K) |
|---|---|---|---|---|---|---|---|
| $8.93\times10^{-9}$ | 0.1 | $1.0\times10^{-5}$ | $1.86\times10^{-9}$ | 1000 | 1000 | 5000 | 7000 |

(a) cement-slag paste with 42% slag, curing temperature 5°C



(b) cement-slag paste with 42% slag, curing temperature 20°C



(c) cement-slag paste with 42% slag, curing temperature 40°C

Fig.4 evaluation of chemically bound water of cement-slag blends

## 4. The evaluation of compressive strength of hardening slag blended concrete

It is well-known that the compressive strength of concrete depends on the gel/space ratio determined from degree of cement hydration and W/C ratio. A gel/space ratio is defined as the ratio of the volumes of the hydrated cement to the sum of the volumes of the hydrated cement and of the capillary pores. For Portland cement pastes, it is approximately assumed that 1 ml of hydrated cement occupies 2.06 ml, and for slag reaction, 1 ml of reacted slag is considered to occupy 2.52 ml of space (Lam *et al.* 2000). So the gel/space ratio of cement-slag blends is given by

$$x_{fc} = \frac{2.06(1/\rho)\alpha C_0 + 2.52(1/\rho_{SG})\alpha_{SG}P}{(1/\rho)\alpha C_0 + (1/\rho_{SG})\alpha_{SG}P + W_0} \tag{13}$$

where $x_{fc}$ is the gel/space ratio of blended cement pastes. It is noted that the volume change of slag is larger than the anhydrous cement (2.52 vs. 2.06). This may be partially due to the lower

density of slag hydration products, and may indicate that slag reaction products are more effective in filling pores (Lam *et al.* 2000).

Furthermore, the development of compressive strength of blended concrete can be evaluated through Powers' strength theory, as

$$f_c = A x_{fc}{}^n \qquad (14\text{-}1)$$

$$A = a1 * \frac{C_0}{C_0 + P} + a2 * \frac{P}{C_0 + P} \qquad (14\text{-}2)$$

$$n = \left( b1 + b2 * \frac{W_0}{C_0 + P} \right) * \frac{C_0}{C_0 + P} + b3 * \frac{P}{C_0 + P} \qquad (14\text{-}3)$$

Where $f_c$ is the compressive strength of blended concrete. $A$ is the intrinsic strength of the material and can be expressed as a function of weight fractions of cement $\left( \dfrac{C_0}{C_0 + P} \right)$ and mineral admixture $\left( \dfrac{P}{C_0 + P} \right)$ in the mixing proportion. The coefficients $a1$ and $a2$ in Eq. (14-2) represent the contributions of cement and mineral admixture to the intrinsic strength of materials, respectively, and the units of *a1*, and *a2* are MPa. *n* is the exponent and also can be expressed as a function of the weight fractions of cement $\left( \dfrac{C_0}{C_0 + P} \right)$ and mineral admixture $\left( \dfrac{P}{C_0 + P} \right)$ in the mixing proportion. The coefficients $\left( b1 + b2 * \dfrac{W_0}{C_0 + P} \right)$ and *b3* in Eq. (14-3) represent the contributions of cement and mineral admixture to strength exponent, respectively. In equation (14-3), $\left( b2 * \dfrac{W_0}{C_0 + P} \right)$ represents the influence of water to binder ratio on strength exponent *n*. In general, given a certain gel-space ratio, compared with cement–slag blends with higher water to binder ratios, the hydration products from lower water to binder ratios show much more homogeneous distributions in both paste matrix zone and interfacial transition zone and lead to more finer pores in the microstructures, which will increase the compressive strength of concrete (Maekawa *et al.* 2009). So in equation (14-3), $b2$ should be higher than zero to reflect this trend.

In this section, the experimental results of compressive strength of slag blended concrete are adopted to verify the proposed model (Cheng *et al.* 2008). The mixing proportions of specimens are shown in Table 3. Water to binder ratios vary between 0.35 and 0.7 (including low strength concrete, moderate strength concrete and high strength concrete), and slag replacement ratios vary from 10% to 40%. Cement content ranges from 177 to 591 kg/m³ according to water–binder ratios.

After casting slag concrete in molds of phi100 × 200 mm cylinders, the cylinders wrapped with plastic film were cured in the chamber at 98 ± 1% humidity and 20℃. Molds were removed after

(a) water to binder ratio 0.35



(b) water to binder ratio 0.5
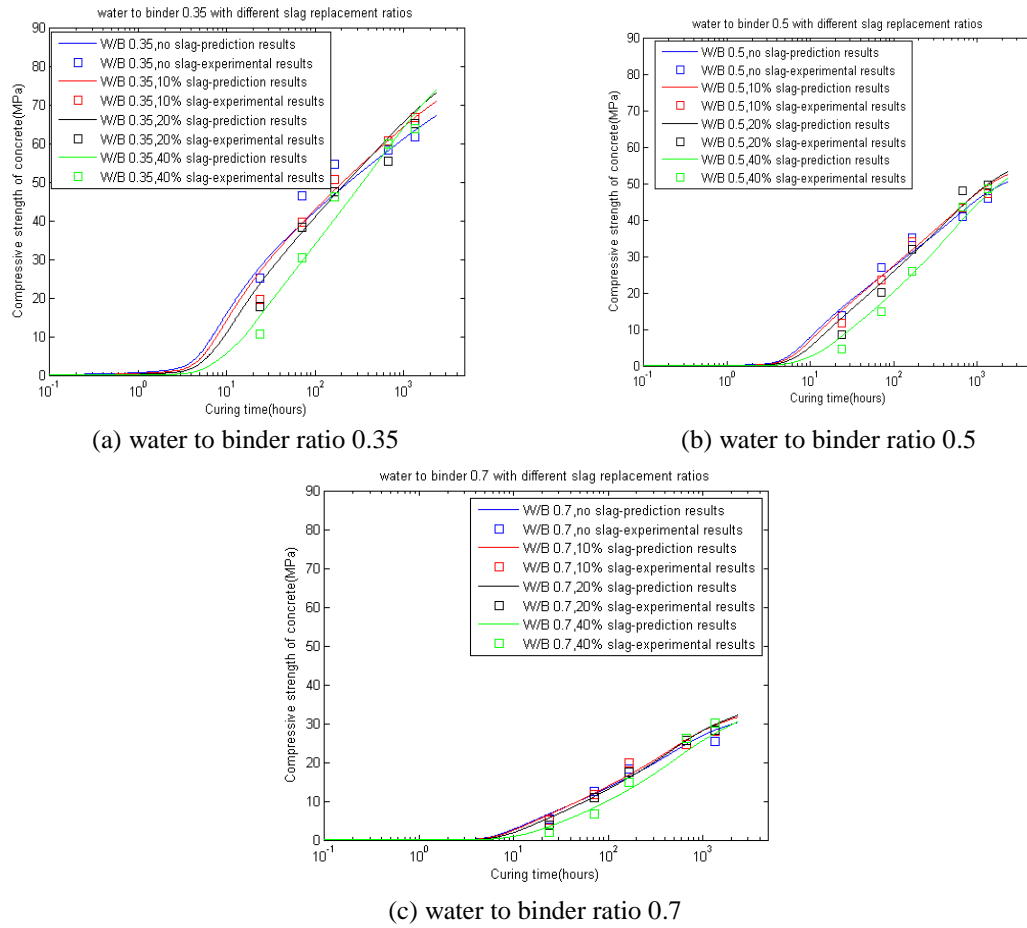


(c) water to binder ratio 0.7

Fig. 5 prediction results of compressive strength of slag blended concrete with different water to binder ratios and slag replacement ratios
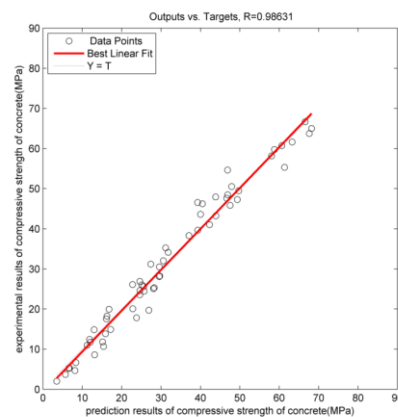


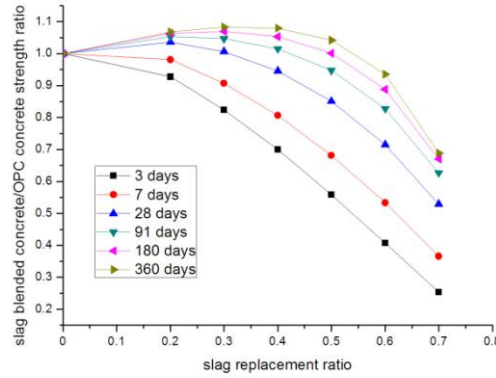Fig. 6 comparison between experimental results and prediction results

Fig. 7 slag blended concrete/OPC concrete strength ratio (water to binder ratio 0.5)

Table 3 Mixing proportions of concrete containing slag

| | Water -to- binder ratio | Slag replacement ratio | Water $(kg/m^3)$ | Cement $(kg/m^3)$ | Slag $(kg/m^3)$ | Sand $(kg/m^3)$ | Aggregate $(kg/m^3)$ | Water reducing agent $(binder \times \%)$ |
|---|---|---|---|---|---|---|---|---|
| WB35 | 0.35 | - | 202.8 | 591 | 0 | 570 | 973 | 4.1 |
| WB35-10 | 0.35 | 10% | 202.8 | 532 | 59 | 565 | 973 | 4.1 |
| WB35-20 | 0.35 | 20% | 202.8 | 473 | 118 | 560 | 973 | 4.1 |
| WB35-40 | 0.35 | 40% | 202.8 | 355 | 236 | 552 | 973 | 4.1 |
| WB50 | 0.5 | - | 206.5 | 414 | 0 | 718 | 973 | 0.4 |
| WB50-10 | 0.5 | 10% | 06.5 | 372 | 41 | 715 | 973 | 0.4 |
| WB50-20 | 0.5 | 20% | 206.5 | 331 | 83 | 712 | 973 | 0.4 |
| WB50-40 | 0.5 | 40% | 206.5 | 248 | 165 | 706 | 973 | 0.4 |
| WB70 | 0.7 | - | 206.9 | 296 | 0 | 815 | 973 | 0 |
| WB70-10 | 0.7 | 10% | 206.9 | 266 | 29 | 815 | 973 | 0 |
| WB70-20 | 0.7 | 20% | 206.9 | 237 | 59 | 812 | 973 | 0 |
| WB70-40 | 0.7 | 40% | 206.9 | 177 | 118 | 807 | 973 | 0 |

48 h and specimens were wet cured at 20℃. The test ages of specimens were 1, 3, 7, 28, and 56 days (including early-age strength and late-age strength).

On the basis of the compressive strength of slag blended concrete, the values of the coefficients of *a1*, *a2*, *b1*, *b2*, and *b3* are regressed as *a1* = 116.95, *a2* = 134.60, *b1* = 1.12, *b2* = 1.61, and *b3*=2.43, respectively. The regression result of *b2* is higher than zero, which agrees with our former assumptions. The comparisons between the experimental results and the prediction results are shown Fig. 5. It is shown that the prediction results generally agree with the experimental results. First, the proposed model shows that given a certain age, with the increasing of water to cement ratio, the compressive strength of Portland cement concrete will decrease correspondingly. Second, the proposed model can reproduce compressive strength crossover phenomenon between control Portland cement concrete and slag blended concrete. The early-age strengths of slag

blended concrete are lower than that of control concrete, and at late age, due to the proceeding of slag reaction, compressive strengths of slag concrete will surpass that of control concrete. With increasing of slag replacement ratios, the reactivity of slag will decrease and the age corresponding to crossover of compressive strength will be postponed. Fig. 6 shows a holistic comparison between experimental results and predicted results. The correlation coefficient between experimental results and predicted results is 0.986 and the root-mean-square error (RMSE) is 3.02 MPa.

Fig. 7 presents parameter analysis about compressive strength development of OPC concrete and slag blended concrete. The water to binder is 0.5, slag replacement ratios vary from 20% to 70%, and the curing ages vary from 3 days to 360 days. The vertical axis represents the strength ratio of slag blended concrete to OPC at the same age. At an early age such as 3 d or 7 d, strength decreases as the slag ratio increases. This may be attributed to the lower reaction degree of slag. As the age increases, obviously the strength of slag blended concrete with higher slag ratios increases faster, and at a late age such as 360 d, the maximum value of strength lies in the range of 40%-50% slag ratios. However, with regards to a slag ratio higher than 50%, due to the lower reaction degree of slag, the ultimate strength ratio is less. Oner and Akyuz (2007) also reported similar experimental results: after an optimum point, at around 50% of the total binder content, the addition of GGBS does not improve the compressive strength.

The summary about determining optimum slag content is shown as follows:

First, using experimental results about hydration degree of cement and reaction degree of slag, calibrate reaction coefficients of cement hydration model and slag reaction model.

Second, using experimental results about compressive strength, calibrate strength development coefficients of slag blended concrete.

Third, make parameter analysis about compressive strength development of Portland cement concrete and slag blended concrete. By comparing the strength development of slag blended concrete with that of Portland cement concrete, the optimum slag content can be analyzed.

In addition, it should be noticed that the coefficients of cement hydration model, slag reaction model, and compressive strength model are not changed with water to binder ratios and slag replacement ratios. It is convenient for other researchers to analyze optimum slag content using the proposed procedure.

As far as the compressive strength is concerned, Bilim *et al.* (2009) used artificial neural networks for predicting the 3, 7, 28, 90, and 360 days compressive strength of concretes containing slag. We should notice that artificial neural networks belong to numerical regression method. A lot of parameters were necessary to build the input layer and hidden layer of artificial neural networks. The physical meaning of these parameters is not clear. Contrastingly, in this paper, the development of compressive strength of slag blended concrete is predicted from the physical aspect, i.e., the development of compressive strength of slag blended concrete is predicted using hydration degree of cement and reaction degree of slag, and is expressed as a function of gel-space ratio, as shown in the Eq. (14). The number of parameters is significantly reduced and the physical meaning of parameters is much clearer than that of artificial neural networks. On the other hand, Papadakis *et al.* (2002) predicted the compressive strengths of matured concrete incorporating different supplementary cementitious materials from the contents of calcium silicate hydrate (CSH). It should be noticed that Papadakis' model is only valid for matured concrete, and can not be used to evaluate the age-dependent properties of concrete. Contrastingly, in this paper, the proposed model is a kinetic model and can be used to evaluate age-dependent properties of hardening blended concrete.

## 5. Conclusions

(1) This paper presents a general procedure to evaluate the development of compressive strength of hardening slag blended concrete. First, by considering the production of calcium hydroxide in cement hydration and its consumption in the slag reaction, a numerical model is proposed to simulate the hydration of concrete containing slag. The degree of hydration of cement and degree of reaction of slag are obtained as accompanied results from the proposed hydration model. Second, on the basis of the volume stoichiometries, mixing proportions of concrete, and the degree of reactions of cement and slag, the gel-space ratio of hydrating blended concrete is calculated. Finally, the development of compressive strength of slag blended concrete is evaluated through Powers' strength theory considering the contributions of cement hydration and slag reaction.

(2) The proposed model can reproduce compressive strength crossover phenomenon between control Portland cement concrete and slag blended concrete. The early-age strengths of slag blended concrete are lower than that of control concrete, and at long term age, due to the proceeding of slag reaction, compressive strengths of slag concrete will surpass that of control concrete. With increasing of slag replacement ratios, the reactivity of slag will decrease and the age corresponding to crossover of compressive strength will be postponed.

(3) The proposed model is valid for low strength slag blended concrete, moderate strength slag blended concrete, and high strength slag blended concrete at both early-age and late age. The proposed model is verified using experimental results including different water to binder ratios (from 0.7 to 0.35) and different slag replacement ratios (10%, 20%, and 40%). After a comparison between experimental results and prediction results, a correlation coefficient 0.986 and a root-mean-square error (RMSE) 3.02 MPa are found. The prediction results show good accordance with the experimental results.

## Acknowledgements

## References

Barnett, S.J., Soutsos, M.N., Millard, S.G. and Bungey, J.H. (2006), "Strength development of mortars containing ground granulated blast-furnace slag: Effect of curing temperature and determination of apparent activation energies", *Cement Concrete Res.*, **36**(3), 434-440.
Bilim, C., Atiş, C.D., Tanyildizi, H. and Karahan, O. (2009), "Predicting the compressive strength of ground granulated blast furnace slag concrete using artificial neural network", *Adv. Eng. Softw.*,**40**(5), 334-340.
Brooks, J.J. and Al-Kaisi, A.F. (1990), "Early strength development of portland and slag cement concretes cured at elevated temperatures", *ACI Mater. J.*, **87**(5), 503-507.
Cheng, A.S., Yen, T., Liu, Y.W. and Sheen, Y.N. (2008), "Relation between porosity and compressive strength of slag concrete", *Structures Congress (edited by Ventura, C., Hoit, M., Anderson, D., Harvey, D.)*, Vancouver, Canada.
De Schutter, G. and Taerwe, L. (1996), "Degree of hydration-based description of mechanical properties of

early age concrete", *Mater. Struct.*, **29**(6), 335-344.

Douglas, E. and Pouskouleli, G. (1991), "Prediction of compressive strength of mortars made with portland cement - blast-furnace slag - fly ash blends", *Cement Concrete Res.*, **21**(4), 523-534.

Han, S.H., Kim, J.K. and Park, Y.D. (2003), "Prediction of compressive strength of fly ash concrete by new apparent activation energy function", *Cement Concrete Res*, **33**(7), 965-971.

Islam, A., Alengaram, U.J., Jumaat, M.Z. and Bashar, II. (2014), "The development of compressive strength of ground granulated blast furnace slag-palm oil fuel ash-fly ash based geopolymer mortar", *Mater. Des.*, **56**(1), 833-841.

Iyoda, T., Inokuchi, K. and Uomoto, T. (2011), "Effect of slag hydration of blast furnace slag cement in different curing conditions", *Proceedings of 13th international congress on the chemistry of cement (edited by Palomo*, *A.*, *Zaragoza*, *A.*, *Agui*, *J.C.L.)*, Madrid.

Lam, L., Wong, Y.L. and Poon, C.S. (2000), "Degree of hydration and gel/space ratio of high-volume fly ash/cement systems ", *Cement Concrete Res.*, **30**(5),747-756.

Luan, Y., Ishida, T., Nawa, T. and Sagawa, T. (2012), "Enhanced model and simulation of hydration process of blast furnace slag in blended cement", *J Adv. Concr. Tech*, **10**(1), 1-13.

Lumley, J.S., Gollop, R.S., Moir, G.K. and Taylor, H.F.W. (1996), "Degrees of reaction of the slag in some blends with Portland cements", *Cement Concrete Res.*, **26**(1), 139-151.

Maekawa, K., Ishida, T. and Kishi, T. (2009), *Multi-scale Modeling of Structural Concrete*, London and New York, Taylor & Francis.

Matsushita, T., Hoshino, S., Maruyama, I., Noguchi, T. and Yamada, K. (2007), "Effect of curing temperature and water to cement ratio on hydration of cement compounds", *Proceedings of 12th international congress on the chemistry of cement (Ed. by Beaudoin, J.)*, Montreal.

Oner, A. and Akyuz, S. (2007), "An experimental study on optimum usage of GGBS for the compressive strength of concrete", *Cement Concrete Compos*, **29**(6), 505-514.

Papadakis, V.G., Antiohos, S. and Tsimas, S. (2002), "Supplementary cementing materials in concrete Part II: A fundamental estimation of the efficiency factor", *Cement Concrete Res.*, **32**(10), 1533-1538.

Saeki, T. and Monteiro, P.J.M. (2005), "A model to predict the amount of calcium hydroxide in concrete containing mineral admixture", *Cement Concrete Res.*, **35**(10), 1914-1921.

Song, H.W. and Kwon, S.J. (2009), "Evaluation of chloride penetration in high performance concrete using neural network algorithm and micro pore structure", *Cement Concrete Res.*, **39**(9),814-824.

Tang, C.W. (2010), "Hydration properties of cement pastes containing high volume mineral admixtures", *Comput. Concr.*, **7**(1),17-38.

Tomosawa, F. (1997), "Development of a kinetic model for hydration of cement", *Proceedings of tenth international congress chemistry of cement (Edited by S. Chandra)*, Gothenburg.

Yoon, I.S. (2009), "Simple approach to calculate chloride diffusivity of concrete considering carbonation", *Comput. Concr.*, **6**(1), 1-18.

*CC*